

*Supporting Information*

**Size and shape evolution of highly magnetic  
iron nanoparticles from successive growth  
reactions**

Andrew J. McGrath<sup>a,b</sup>, Soshan Cheong<sup>c</sup>, Anna M. Henning<sup>d</sup>, J. Justin  
Gooding<sup>a,b,e</sup> and Richard D. Tilley<sup>a,b,c</sup>

a. School of Chemistry, University of New South Wales, NSW 2052, Australia.

b. Australian Centre for Nanomedicine, University of New South Wales, NSW 2052, Australia.

c. Electron Microscope Unit, Mark Wainwright Analytical Centre, University of New South Wales, NSW 2052, Australia.

d. Boutiq Science Ltd and Ferronova Pty Ltd, Victoria University of Wellington, Wellington 6012, New Zealand

e. ARC Centre for Convergent Bio-Nanoscience and Technology, University of New South Wales, NSW 2052, Australia

## **Experimental**

*Chemicals used:* Ferrocene (98%), aluminium chloride (99%), benzene (anhydrous, 99.8%), aluminium powder (complexometric, >91%), potassium hexafluorophosphate (98%), lithium aluminium chloride (95%), mesitylene (98%) and oleylamine (OLA, >98% primary amine) were purchased from Sigma Aldrich. THF (99.9%) was purchased from ChemSolute. All chemicals were used as-received.

*Synthesis of 7 nm iron seeds:* The iron precursor  $\text{Fe}(\text{C}_5\text{H}_5)(\text{C}_6\text{H}_7)$  was synthesized using known methods.<sup>1</sup> In a typical synthesis of iron seeds,  $\text{Fe}(\text{C}_5\text{H}_5)(\text{C}_6\text{H}_7)$  (0.3 g, 0.75 mmol) was dissolved in mesitylene (6 mL), which was degassed prior by bubbling through  $\text{N}_2$  for 20 minutes. To this solution, OLA (1.5 mL, 2.3 mmol) was added, the reaction mixture sonicated briefly, and then degassed under vacuum and nitrogen for a total of three cycles. The solution was then transferred to a 10 oz. Fischer Porter bottle, and degassed with three cycles of hydrogen and vacuum. The bottle was finally pressurised with 3 bar hydrogen gas, and left in an oven at 110 °C to react for 72 hr. The bottle was then allowed to cool to room temperature, and the hydrogen gas evacuated under vacuum at the Schlenk line. The bottle was then transferred to a nitrogen-filled glovebox, opened, and the reaction solution set aside.

*Seed-mediated synthesis of 10, 11 and 13 nm iron nanoparticles:* A reaction solution consisting of  $\text{Fe}(\text{C}_5\text{H}_5)(\text{C}_6\text{H}_7)$  (0.3 g, 0.75 mmol), OLA (0.5 mL, 0.75 mmol) and mesitylene (6 mL) was made up in the glovebox. To this solution, 2 mL of the previously-synthesized 7 nm seed solution was added without purification. The final [seed]:[precursor] molar Fe ratio was 1:5. The solution was transferred to a Fischer Porter bottle, sonicated briefly, degassed under hydrogen and vacuum, and then pressurized with 3 bar hydrogen gas and left to react in an oven at 110 °C for 24 hr. The bottle was allowed to cool to room temperature, the hydrogen evacuated under vacuum at the Schlenk line, and the bottle transferred to the glovebox, where the reaction solution was stored. An aliquot of this sample was taken for further characterization, and nanoparticles were recovered via centrifugation at 4000 rpm, followed by washing with toluene:OLA (10:1 v/v) and suspension in toluene.

The synthetic protocol for further growth reactions was the same as that for 10 nm iron nanoparticles, however for 11 nm nanoparticles, 10 nm iron nanoparticles were used as seeds, and for 13 nm nanoparticles, 11 nm iron nanoparticles were used as seeds. In each case, seeds were added from their raw reaction solution to a final [seed]:[precursor] molar Fe ratio of 1:5.

*TEM analysis:* Samples for TEM were prepared by drop-casting a solution of iron nanoparticles suspended in toluene onto a carbon-coated copper grid. Low- and high-resolution transmission electron microscopy (TEM) images were taken on a JEOL 2100F microscope operating at an accelerating voltage of 200 kV. For HRTEM images, TEM grids were cleaned via plasma cleaning (15 min, 300 V) to remove excess surfactant.

*XRD analysis:* Samples for X-ray diffraction (XRD) analysis of the iron nanoparticles were prepared via dropping a chloroform dispersion of the as-synthesized nanoparticles onto an amorphous silicon substrate, and leaving the dispersion to dry in open air. Powder XRD measurements were obtained from a Pan Analytical X'pert Pro MPD X-ray diffraction System using Cu K $\alpha$  radiation.

*Magnetic measurements:* A dispersion of the iron nanoparticles was dried under vacuum and the powder transferred to a gelatin capsule under ambient conditions. The capsule was sealed, and the sample inserted into a vibrating sample magnetometer attached to a Quantum Design Physical Property Measurement System. All measurements were taken at 300 K.

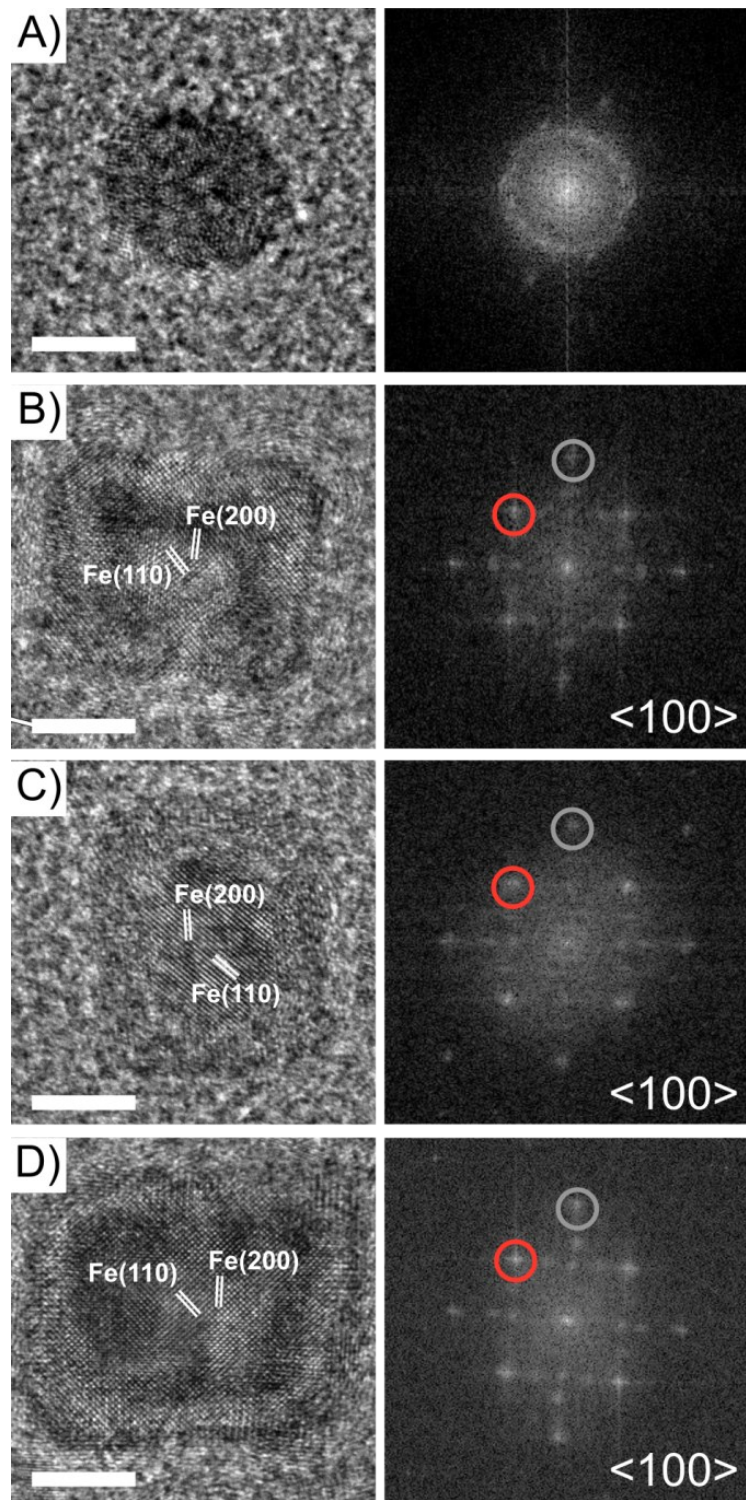


**Figure S1.** HRTEM images of A) 7 nm oxidized Fe seeds, and B) 10 nm, C) 11 nm, and D) 13 nm iron/iron oxide nanoparticles, with corresponding fast Fourier transform (FFT) power spectra displayed beside the according HRTEM image. Lattice fringes corresponding to  $\alpha$ -Fe are indicated in the HRTEM images, where observed. The red circles in the FFT spectra indicate spots corresponding to (110) signals and grey circles correspond to (200) signals, from  $\alpha$ -Fe. Scale bars correspond to 5 nm.

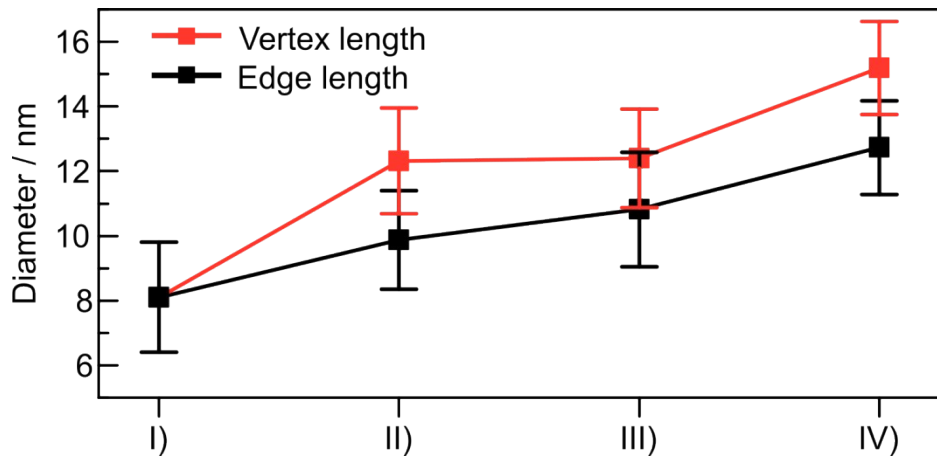


**Figure S2.** Plot of nanoparticle diagonal diameter (“vertex length”) and of face-to-face diameter (“edge length”) with increasing growth reactions. Stage I corresponds to the Fe nanoparticle seeds, and stage II-IV corresponds to iron nanoparticles obtained after one, two and three growth reactions, respectively.

**Table S1.** Comparison of iron nanoparticle sizes at different stages, across the nanoparticle diagonal diameter (“vertex length”) and of face-to-face diameter (“edge length”).

Stage	Vertex length	Edge length
I	$7.4 \pm 1.3$	$7.4 \pm 1.3$
II	$12.3 \pm 1.6$	$9.9 \pm 1.5$
III	$12.4 \pm 1.5$	$10.8 \pm 1.8$
IV	$15.2 \pm 1.4$	$12.7 \pm 1.5$

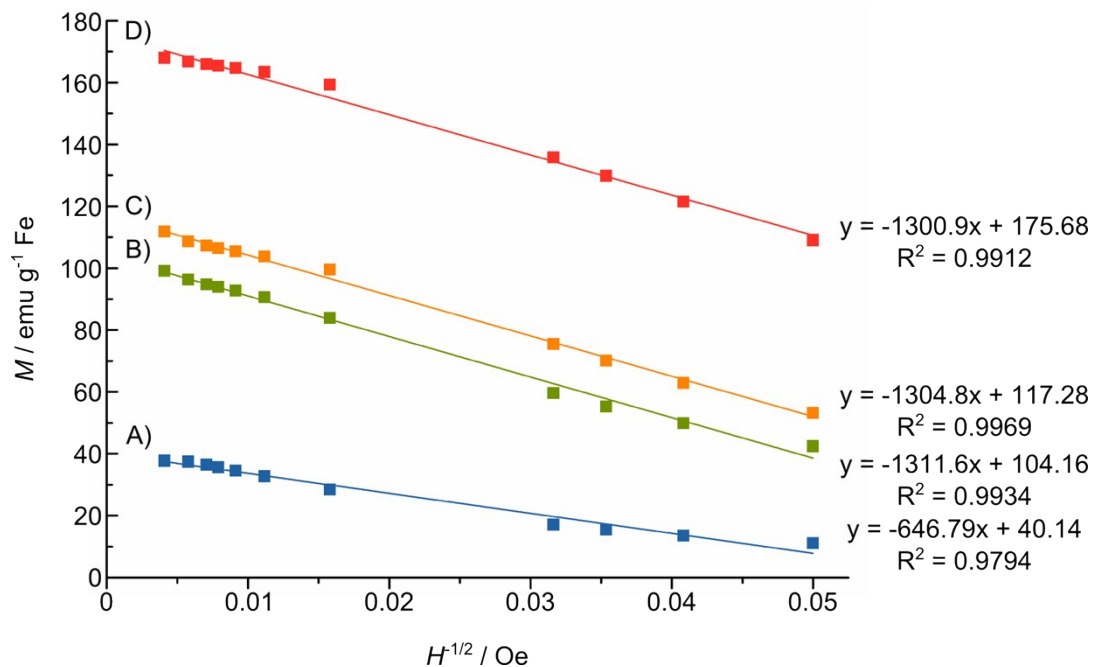


**Figure S3.** Plots of  $M$  against  $H^{-1/2}$ , with the linear fit extrapolated to  $H^{-1/2} = 0$  to give calculated  $M_s$  for A) 7 nm, B) 10 nm, C) 11 nm and D) 13 nm iron/iron oxide nanoparticles.

**Table S2.** Comparisons of  $M_s$  (by mass of Fe) at 300 K for iron/iron oxide core/shell nanoparticles reported in the literature.

Reference	Size (nm)	Shape	$M_s$ (emu g <sup>-1</sup> Fe)
2	10	Cubic	101 <sup>a</sup>
3	9	Spherical	106
4	12.5	Spherical	121
5	14	Spherical	148
6	16	Spherical	150
7	10	Spherical	163
8	15	Spherical	164 <sup>a</sup>
This work	13	Cubic	176

<sup>a</sup> Converted to emu g<sup>-1</sup> Fe from units of A m<sup>2</sup> kg<sup>-1</sup> Fe.

## References

- (1) M. L. H. Green, L. Pratt and G. Wilkinson, *J. Chem. Soc. Dalt. Trans.*, 1960, 989-997.
- (2) A. Shavel, B. Rodríguez-González, M. Spasova, M. Farle and L. M. Liz-Marzan, *Adv. Funct. Mater.*, 2007, **17**, 3870-3876.
- (3) S. Peng, C. Wang, J. Xie, and S. Sun, *J. Am. Chem. Soc.*, 2006, **128**, 10676-10677.
- (4) S. Zhang, G. Jiang, G. Filsinger, L. Wu, H. Zhu, J. Lee, Z. Wu and S. Sun, *Nanoscale*, 2014, **6**, 4852-4856.
- (5) D. A. J. Herman, P. Ferguson, S. Cheong, I. F. Hermans, B. J. Ruck, K. M. Allan, S. Prabakar, J. L. Spencer, C. D. Lendrum and R. D. Tilley, *Chem. Commun.*, 2011, **47**, 9221-9223.
- (6) S. Cheong, P. Ferguson, K. W. Feindel, I. F. Hermans, P. T. Callaghan, C. Meyer, A. Slocombe, C.-H. Su, F.-Y. Cheng, C.-S. Yeh, B. Ingham, M. F. Toney and R. D. Tilley, *Angew. Chem. Int. Ed.*, 2011, **50**, 4206-4209.
- (7) H. Kura, M. Takahashi and T. Ogawa, *J. Phys. Chem. C*, 2010, **114**, 5835-5838.
- (8) L.-M. Lacroix, N. F. Huls, D. Ho, X. Sun, K. Cheng and S. Sun, *Nano Lett.*, 2011, **11**, 1641-1645.